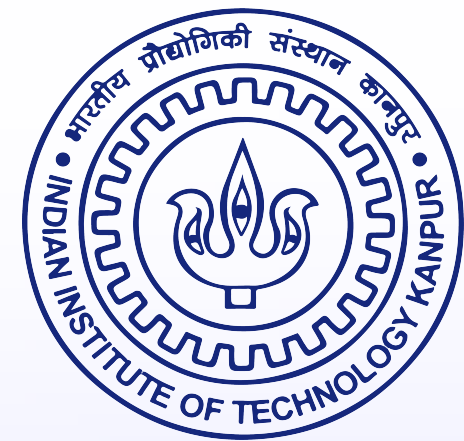


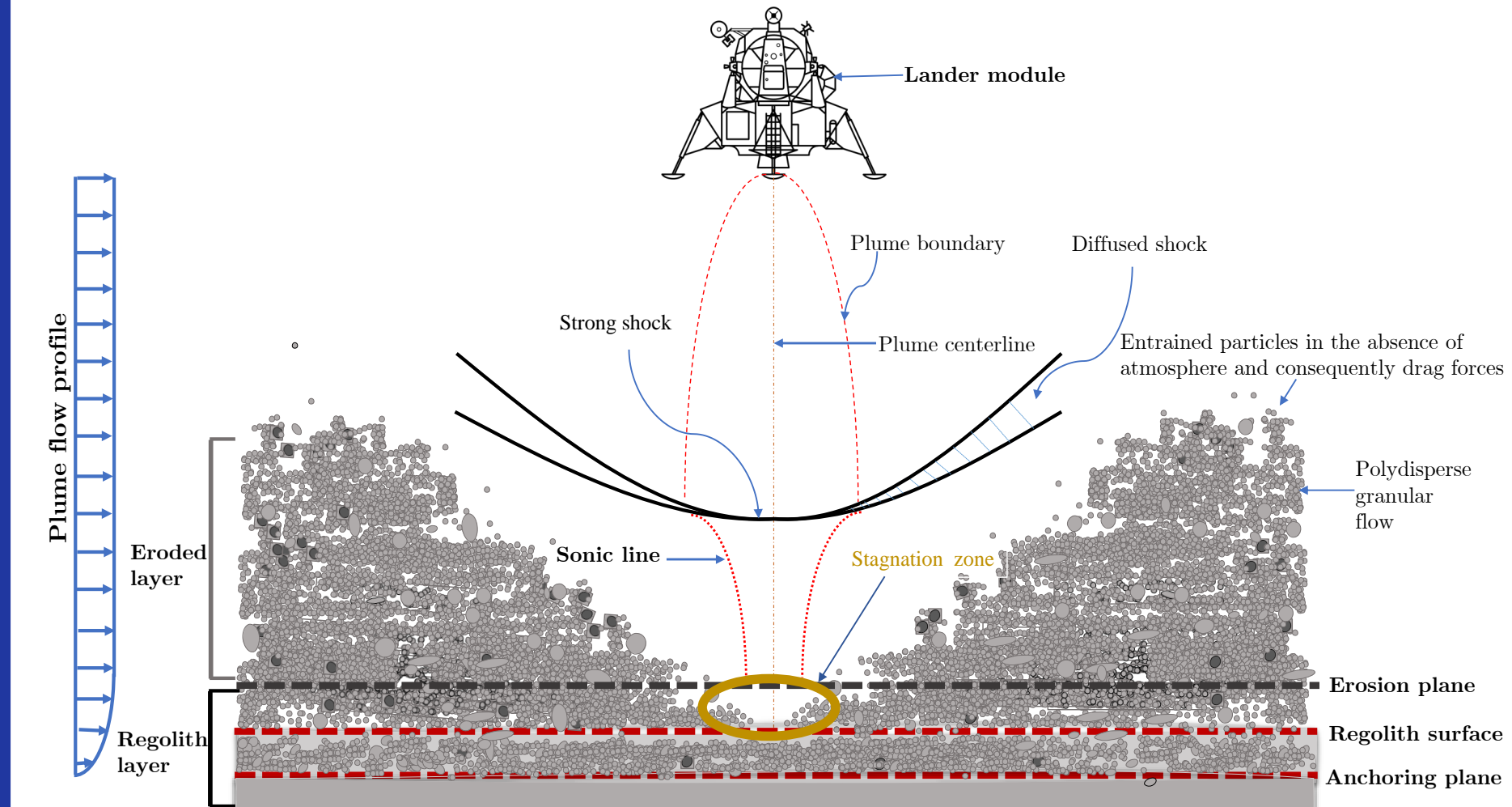
Plume Surface Interaction During Lunar Landing



Aasheesh Bajpai, Ashish Bhateja, Rakesh Kumar
aasheesh@iitk.ac.in, ashish@iitgoa.ac.in, rkm@iitk.ac.in

Lunar Landing Problem

Dust is the number one concern in returning to the moon.



Flowchart

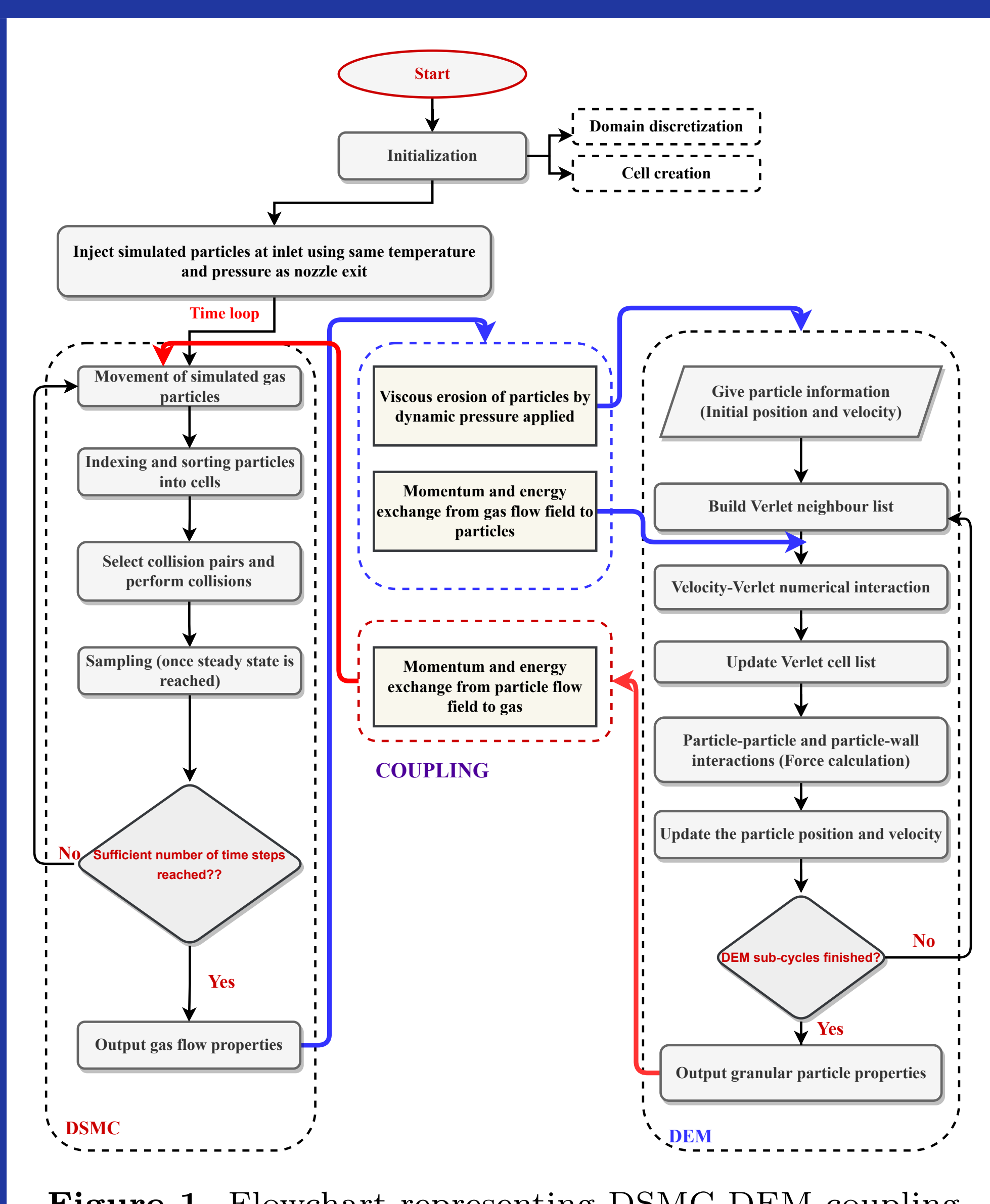


Figure 1. Flowchart representing DSMC-DEM coupling algorithm.

Schematic

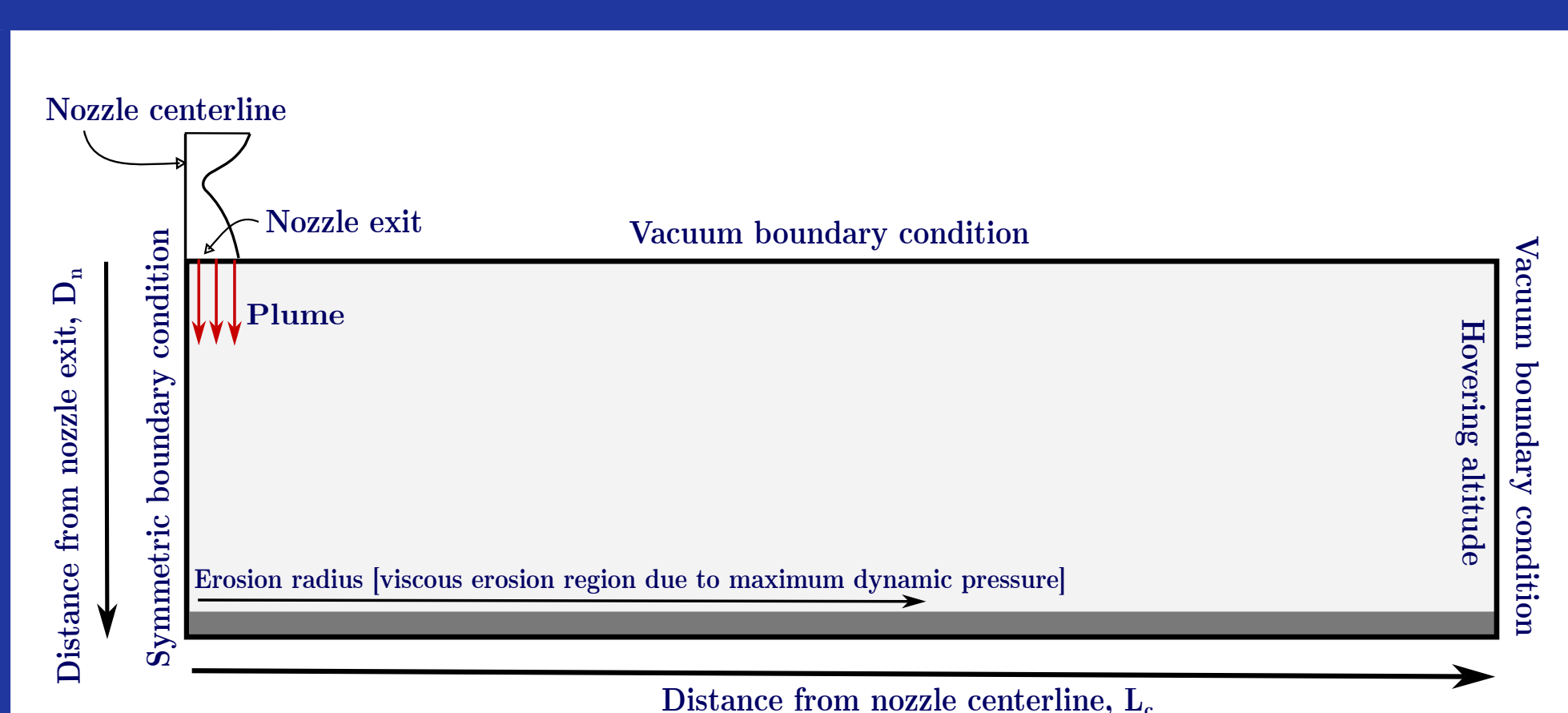


Figure 2. Schematic view of plume impingement on a lunar surface.

Methodology

It is very challenging computationally to run gas and grain phase simulations simultaneously due to huge differences in the relaxation time of each phase. Therefore, we have performed two way coupled Lagrangian-Lagrangian simulation in stage-wise manner.

Stage 1: Simulation of flow through nozzle using NFS DSMC solver and nozzle exit properties will be extracted.

Stage 2: Nozzle exit properties will be used as input to the gas phase solver, which will simulate plume impingement on the planetary body without considering erosion. Gas flow field will be obtained for the domain.

Stage 3: Keeping the gas-phase flow-field unchanged, we will obtain grain phase results by running the gas-grain solver. Here, grain-grain collisions will be handled by DEM solver, while gas-grain interactions will be modeled in the modified DSMC framework.

Stage 4: Gas-phase simulation using gas-grain solver will continue from the same time step where it ends in stage 2 to obtain updated gas-phase properties in the background of grain phase data.

Stage 5: The final results are obtained for the grain phase by re-running the gas-grain solver in the gas background with updated gas-phase results from stage 4.

Stage 1: Nozzle

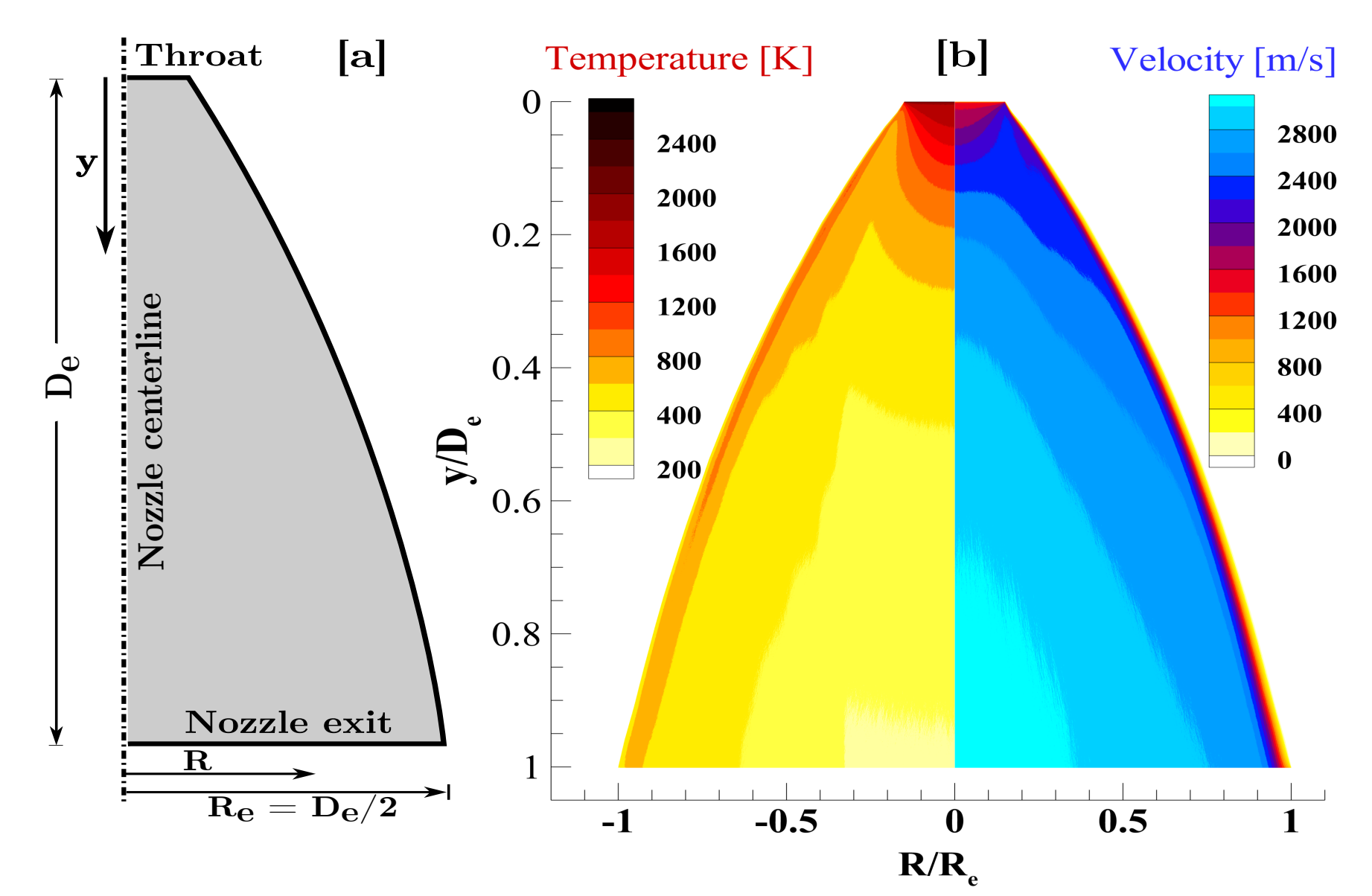


Figure 3. [a] Schematic of a nozzle. [b] Temperature and velocity contours of the flow field in the nozzle. Here D_e and R_e represent the diameter and radius of the nozzle exit, respectively.

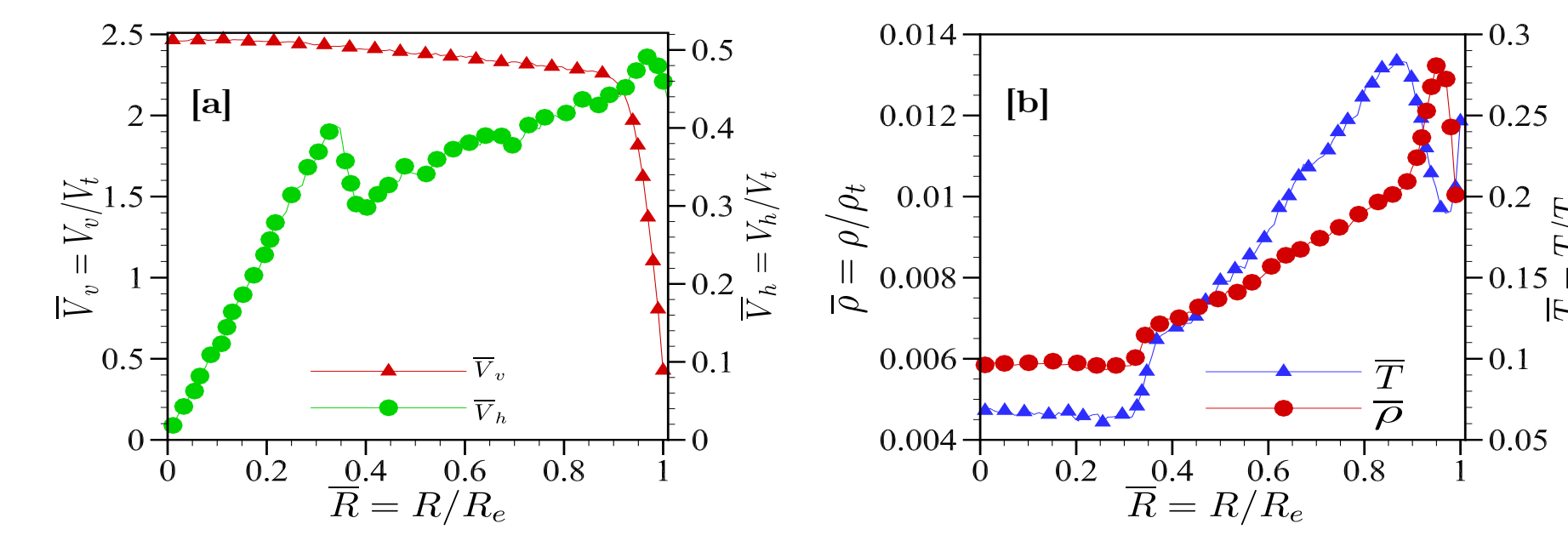


Figure 4. Variation of flow properties at the nozzle exit. (a) Normalised vertical and horizontal velocities, and (b) normalised density and temperature.

Stage 2: Plume Impingement

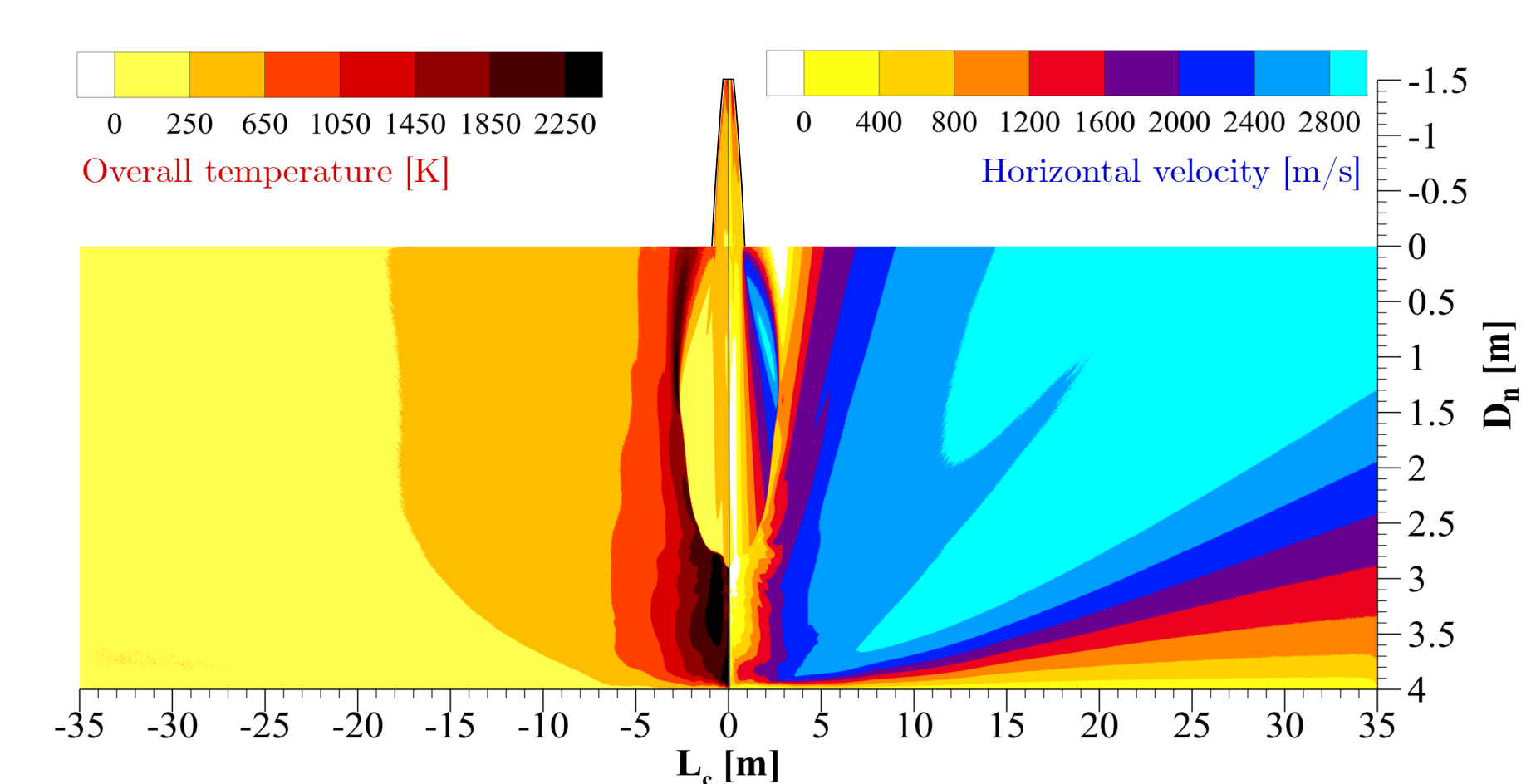


Figure 5. Spatial distribution of the horizontal velocity and overall temperature for the entire domain.

Viscous Erosion

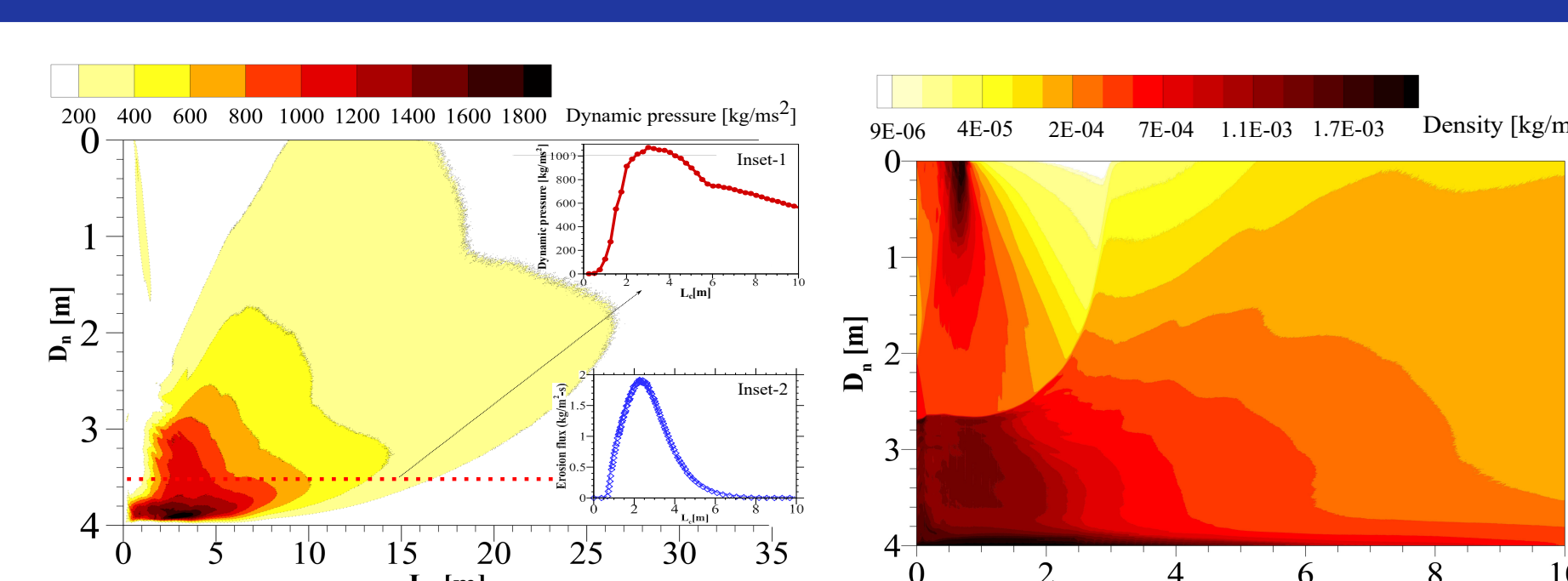


Figure 6. Contours representing the dynamic pressure responsible for erosion. Inset-1: Dynamic pressure variation at the depth of 3.5 m below nozzle exit. Inset-2: Erosion flux variation at the lunar surface.

Stage 3: Lunar Particles

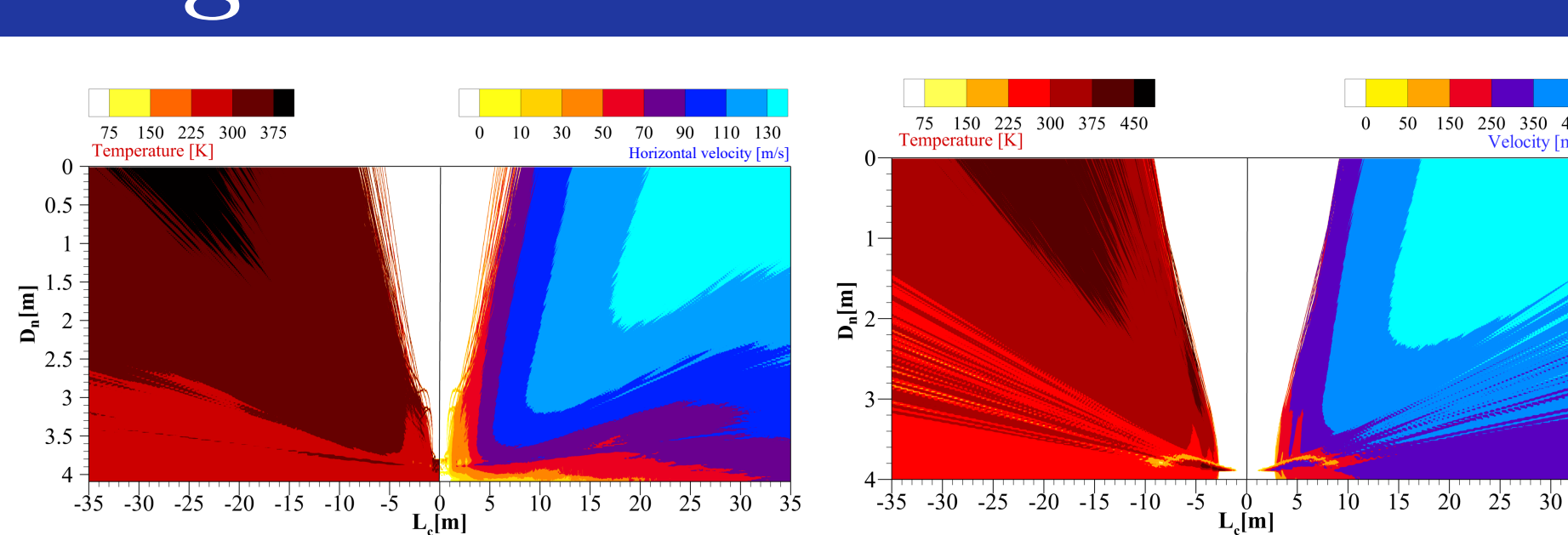


Figure 7. Spatial distribution of horizontal velocity and temperature for $1000 \mu\text{m}$ diameter and $100 \mu\text{m}$ diameter particles.

Particle Flow Field

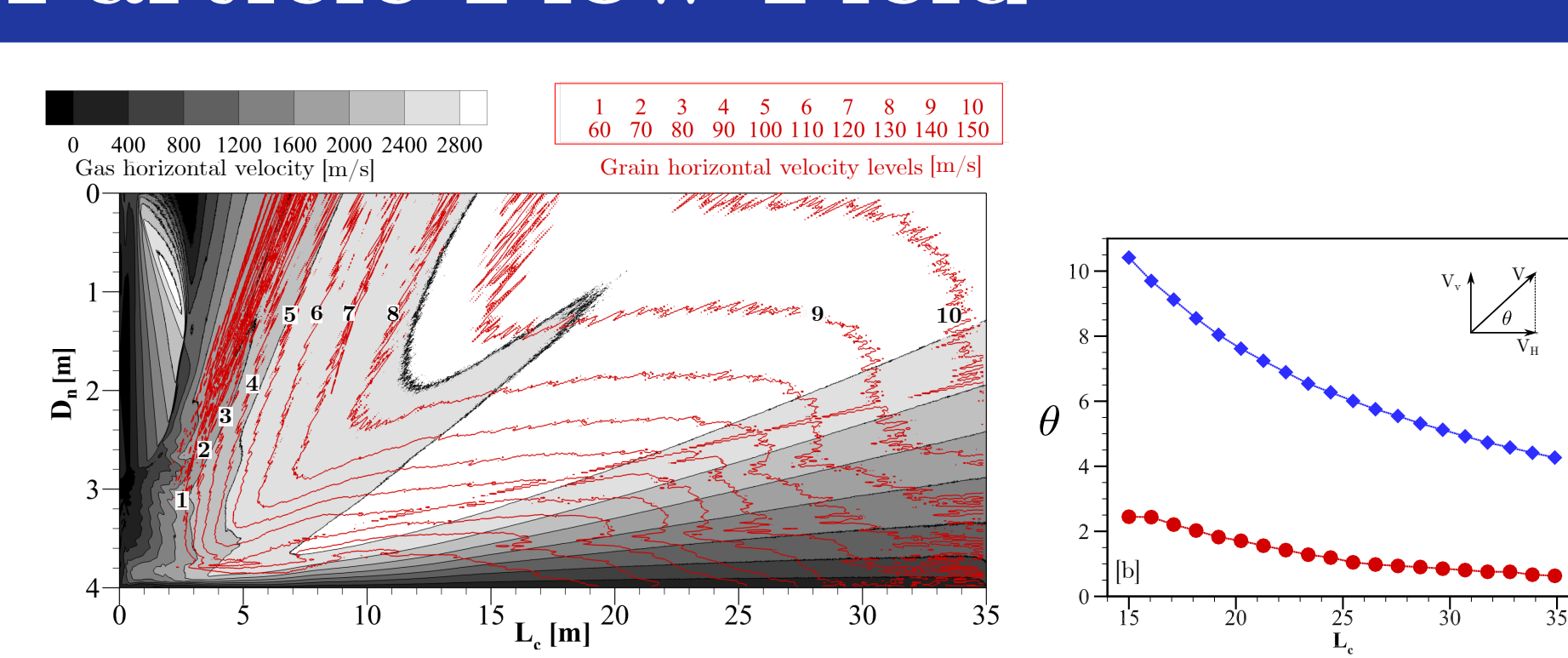


Figure 8. [a] The horizontal velocity contours of the gas and grain phase and [b] Variation of inverse tangential of V_v/V_H in degrees, at two depths from the nozzle exit.

Particle Trajectory

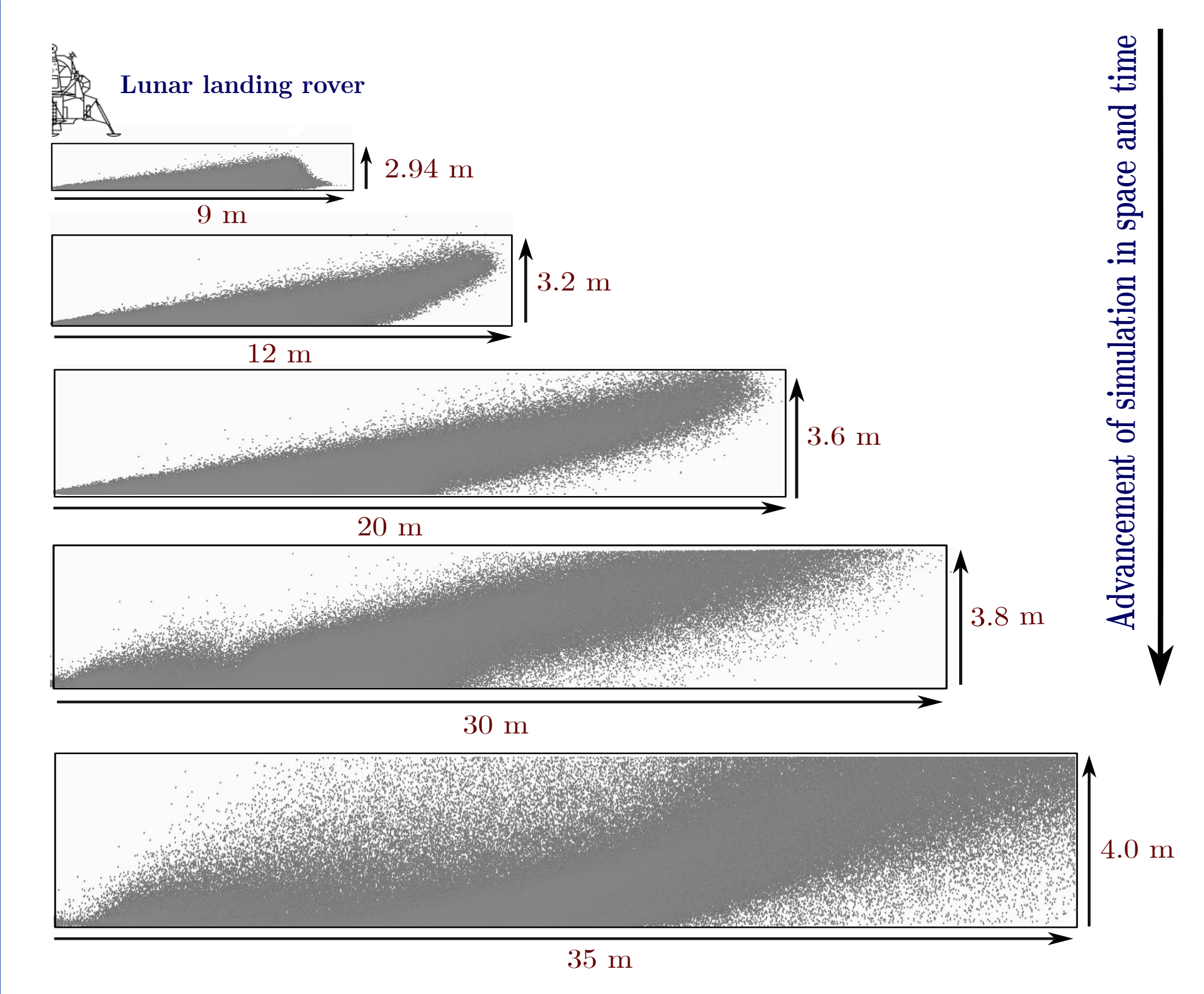


Figure 9. Trajectories of lunar particles at different time instants.

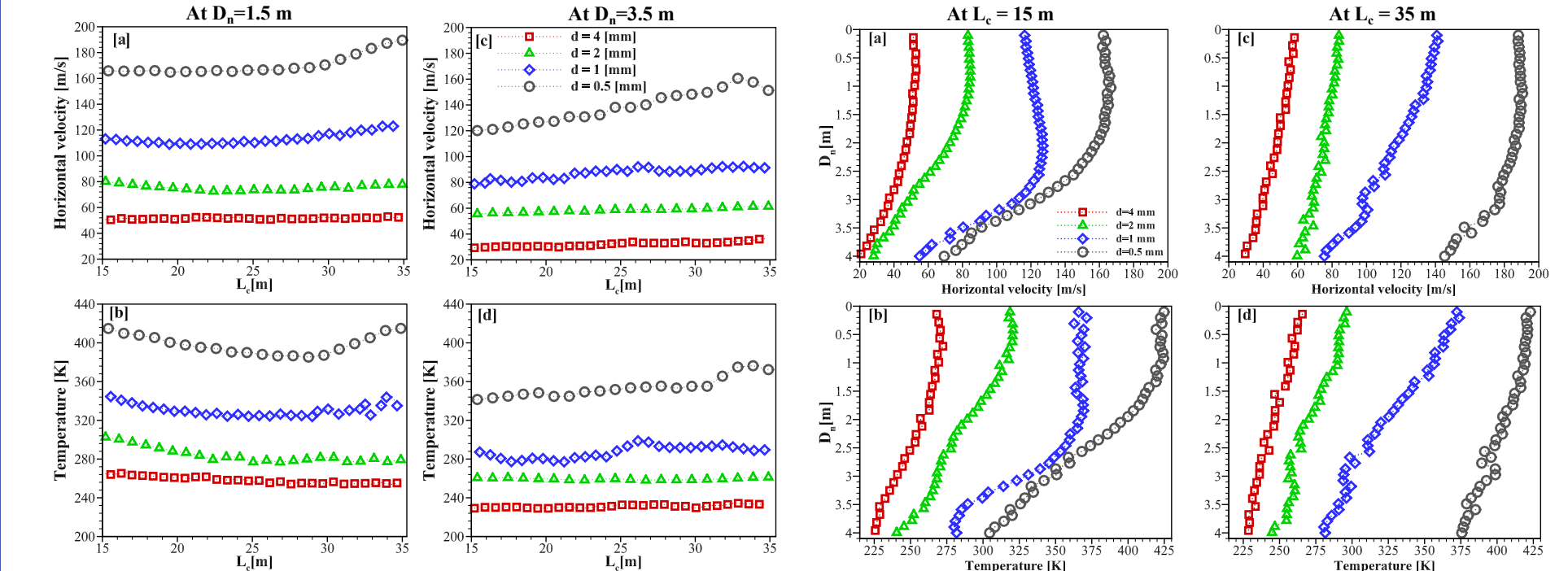


Figure 10. Horizontal velocity and temperature variations for two depths from the nozzle exit and different far-field locations from the nozzle centerline.

Stage 4: Two Way Coupling (Gas Phase)

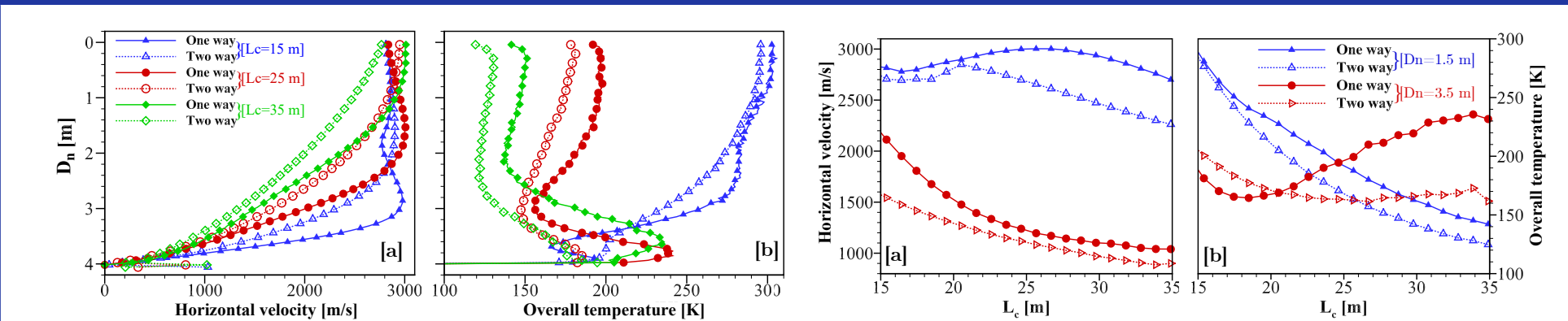


Figure 11. Horizontal velocity and temperature variations for two depths from the nozzle exit and different far-field locations from the nozzle centerline.

Stage 5: Two Way Coupling (Grain Phase)

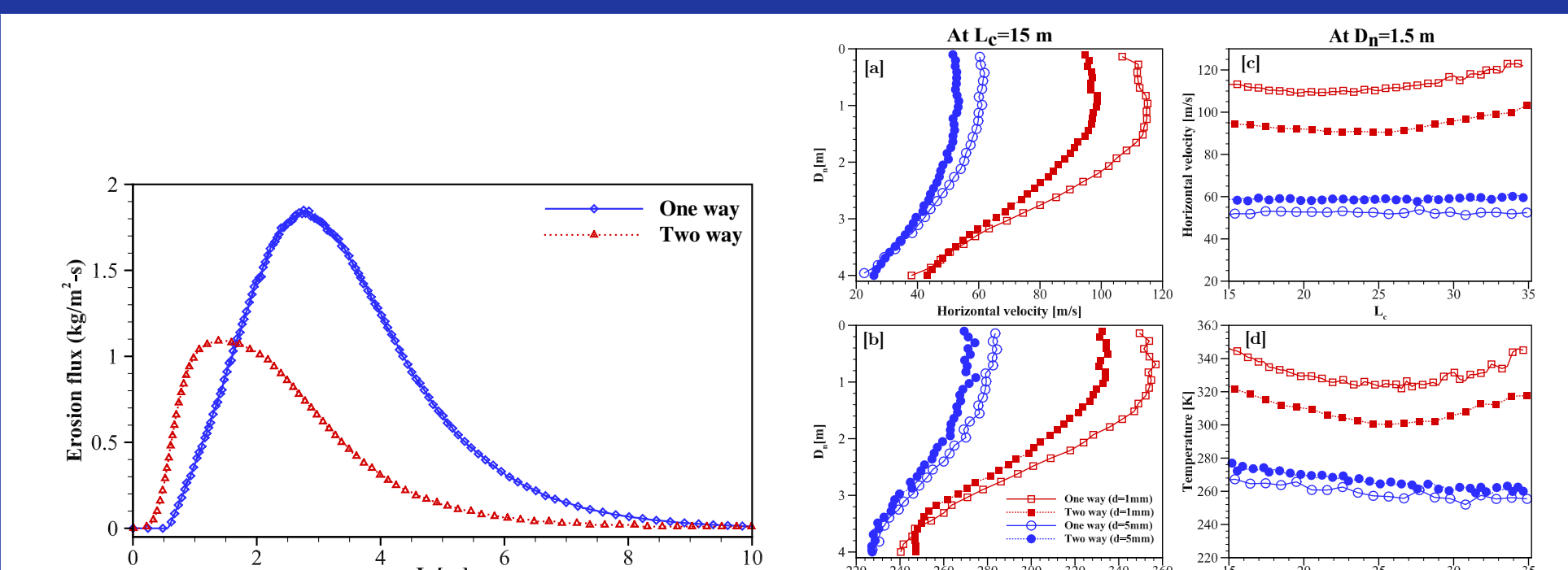


Figure 12. Erosion flux comparison and, comparison of horizontal velocity and temperature variations for 15 m far-field distance from nozzle centerline and 1.5 m depth below the nozzle exit.

Conclusions

- The developed framework can be used in the future to study any type of particle, even with the larger size, shape and frictional properties.
- The simulations yielded a particle velocity range spanning from 50 m/s to 450 m/s, corresponding to particle sizes ranging from 5 mm to 100 μm respectively, observed at a distance of 15 m from the nozzle centerline. The corresponding range of angles for particle trajectories was found to vary from 2° to 15° for all particle sizes.
- The study analyzed the impact of grain properties on the gas flow field and vice versa. It was observed that the gas flow field experiences a loss of momentum and energy upon interacting with grains, leading to a decrease in gas velocity and temperature. As a result, there is a significant change in dynamic pressure, contributing to a reduction in the number of eroded grain particles.
- Particle size significantly influences trajectory and properties. Larger particles result in decreased peak grain velocity and temperature.

Acknowledgements

The authors thank the Science and Engineering Research Board (SERB) for financial support (Grant No. CRG/2019/003989) and the National Supercomputing Mission (NSM) for access to computing resources on "PARAM Sanganak" at IIT Kanpur.